

Università degli Studi di Napoli “Federico II”



**SCUOLA POLITECNICA E DELLE SCIENZE DI BASE
DIPARTIMENTO DI INGEGNERIA INDUSTRIALE**

**CORSO DI LAUREA IN INGEGNERIA AEROSPAZIALE
CLASSE DELLE LAUREE IN INGEGNERIA INDUSTRIALE (L-9)**

Elaborato di laurea in Meccanica del Volo
**Geometric modelling, analysis of performance,
stability and control of turboprop military
transport aircraft**

**Relatore:
Prof. Danilo Ciliberti**

**Candidato:
Guido Ricci
Matr. N35003513**

ANNO ACCADEMICO 2022 – 2023

*Alla mia famiglia,
Ai miei amici,
A tutti gli ostacoli superati.*

Abstract

The purpose of this work is the geometric modelling, analysis of performance, stability and control of two turboprop transport military aircraft: the C-27J Spartan and the C-130 Hercules. The modelling phase was carried out with JPAD Modeller, a software that supports the design of aircraft ensuring the designer useful tools for the whole process offering the possibility to recreate the model more likely to the real counterpart thanks to a high possibility of customization of the components. Then the analysis of performance was carried out using MATLAB, software for numerical calculation and statistical analysis. To conduct the analysis, codes that included information on the size, engines and consumption of the two aircraft were made and then these codes were added to a live script that displays the performance values. At the end, the analysis of stability and control was implemented through OpenVSP, software to make 3D models and perform engineering analysis on these. For stability and control, after importing the models from JPAD Modeller, it was used the VSPAERO tool that applies discrete vortices on the aircraft panels, evaluating them over the entire surface returning a pressure distribution and then a distribution of aerodynamic forces.

Sommario

Il presente lavoro ha come fine la modellazione geometrica, l'analisi delle prestazioni, della stabilità e del controllo di due velivoli da trasporto militare turboprop: il C-27J Spartan e il C-130 Hercules. La fase di modellazione è stata effettuata tramite JPAD Modeller, un software che supporta la progettazione di aeromobili garantendo al progettista strumenti utili per l'intero processo offrendo la possibilità di ricreare il modello più verosimilmente alla controparte reale grazie ad una elevata possibilità di personalizzazione delle componenti. Successivamente è stata effettuata l'analisi delle prestazioni tramite MATLAB, software per il calcolo numerico e l'analisi statistica. Per realizzare l'analisi sono stati creati dei codici nei quali sono stati immessi dati in merito alle dimensioni, motori e consumi dei due velivoli; i codici ottenuti sono stati inseriti in un live script che restituisce in output i valori delle performance. Infine l'analisi della stabilità e controllo è stata attuata tramite OpenVSP, software per realizzare modelli 3D ed effettuare analisi ingegneristiche su questi. Per la stabilità e il controllo, dopo aver importato i modelli da JPAD Modeller, è stato utilizzato il tool VSPAERO che applica vortici discreti sui pannelli del velivolo, valutandoli sull'intera superficie restituendo una distribuzione di pressione e quindi una distribuzione delle forze aerodinamiche.

Table of contents

| | |
|--|----|
| 1. Introduction | 7 |
| 1.1 Objectives | 7 |
| 1.2 Layout of work..... | 7 |
| 1.3 C-27J Spartan..... | 8 |
| 1.4 C-130 Hercules | 9 |
| 2. Aircraft components..... | 10 |
| 2.1 Fuselage | 10 |
| 2.2 Wing..... | 11 |
| 2.2.1 Wing planform parameters | 11 |
| 2.2.2 Ailerons | 12 |
| 2.2.3 Flaps and Slats | 12 |
| 2.3 Tail..... | 13 |
| 2.3.1 Horizontal Tail..... | 13 |
| 2.3.2 Vertical Tail..... | 13 |
| 2.4 Engine | 14 |
| 2.4.1 Turboprop engine | 14 |
| 3. Geometric modelling..... | 16 |
| 3.1 Data..... | 17 |
| 3.1.1 C-27J Spartan | 17 |
| 3.1.2 C-130 Hercules | 18 |
| 3.2 Geometric modelling process | 18 |
| 3.3 C-27J Spartan geometric modelling | 19 |
| 3.4 C-130 Hercules geometric modelling | 23 |

| | | |
|-----|---|----|
| 4. | Analysis of performance | 27 |
| 4.1 | Input data | 27 |
| 4.2 | Technical Polar | 28 |
| 4.3 | Propulsive characteristics | 33 |
| 4.4 | Climb, level flight, autonomies, take-off and landing distances | 33 |
| 4.5 | Turn..... | 35 |
| 5. | Analysis of stability and control..... | 36 |
| 5.1 | Aerodynamic stability derivatives | 40 |
| 5.2 | Neutral point and static stability margin..... | 41 |
| 6. | Conclusion..... | 42 |

List of figures

| | |
|--|----|
| Figure 1.1 - The Italian Air Force C-27J Spartan..... | 8 |
| Figure 1.2 - C-130 Hercules..... | 9 |
| Figure 2.1 - Fuselage structure..... | 10 |
| Figure 2.2 - Principal wing planform parameters..... | 11 |
| Figure 2.3 - Wing Dihedral angle..... | 12 |
| Figure 2.4 - Ailerons operation..... | 12 |
| Figure 2.5 - Flaps and slats..... | 13 |
| Figure 2.6 - Horizontal and vertical tails..... | 14 |
| Figure 2.7 - Scheme of turboprop engine..... | 15 |
| Figure 3.1 - JPAD Modeller key visual..... | 16 |
| Figure 3.2 - C-27J Spartan isometric view..... | 19 |
| Figure 3.3 - C-27J Spartan CAD model views..... | 19 |
| Figure 3.4 - Comparison of C-27J Spartan line drawings..... | 20 |
| Figure 3.5 - C-27J Spartan ailerons operation (-25°, 0°, +25°) | 21 |
| Figure 3.6 - C-27J Spartan elevator operation (-25°, 0°, +25°) | 21 |
| Figure 3.7 - C-27J Spartan rudder operation (-30°, 0°, +30°) | 22 |
| Figure 3.8 - C-27J Spartan flaps operation (0°, +45°) | 22 |
| Figure 3.9 - C-130 Hercules isometric view..... | 23 |
| Figure 3.10 - C-130 Hercules CAD model views..... | 23 |
| Figure 3.11 - Comparison of C-130 Hercules line drawings..... | 24 |
| Figure 3.12 - C-130 Hercules ailerons operation (-25°, 0°, +25°) | 25 |
| Figure 3.13 - C-130 Hercules elevator operation (-25°, 0°, +25°) | 25 |
| Figure 3.14 - C-130 Hercules rudder operation (-30°, 0°, +30°) | 26 |
| Figure 3.15 - C-130 Hercules flaps operation (0°, +45°) | 26 |
| Figure 4.1 - C-27J Spartan Technical polar results..... | 32 |
| Figure 4.2 - C-130 Hercules Technical polar results..... | 32 |
| Figure 4.3 - C-27J Spartan diagram of required and available power..... | 34 |
| Figure 4.4 - C-130 Hercules diagram of required and available power..... | 34 |
| Figure 5.1 - OpenVSP user interface..... | 36 |
| Figure 5.2 - The two aircraft models in OpenVSP..... | 37 |

List of tables

| | |
|---|----|
| Table 3.1 - C-27 J technical data..... | 17 |
| Table 3.2 - C-130 Hercules technical data..... | 18 |
| Table 4.1 - Aerodynamic data..... | 27 |
| Table 4.2 - Weight and geometric data..... | 28 |
| Table 4.3 - Powerplant data..... | 28 |
| Table 4.4 - Point E, Sea Level..... | 29 |
| Table 4.5 - Point P, Sea Level..... | 29 |
| Table 4.6 - Point A, Sea Level..... | 29 |
| Table 4.7 - Point S, Sea Level..... | 29 |
| Table 4.8 - Point E, Climb Level..... | 30 |
| Table 4.9 - Point P, Climb Level..... | 30 |
| Table 4.10 - Point A, Climb Level..... | 30 |
| Table 4.11 - Point S, Climb Level..... | 30 |
| Table 4.12 - Point E, Cruise Level..... | 31 |
| Table 4.13 - Point P, Cruise Level..... | 31 |
| Table 4.14 - Point A, Cruise Level..... | 31 |
| Table 4.15 - Point S, Cruise Level..... | 31 |
| Table 4.16 - Propulsive Characteristics..... | 33 |
| Table 4.17 - Climb, level flight, autonomies, Take-off and Landing distances..... | 33 |
| Table 4.18 - Turn..... | 35 |
| Table 5.1 - C-27J Spartan C_L , C_M and C_N results obtained by the solver in several cases..... | 38 |
| Table 5.2 - C-130 Hercules C_L , C_M and C_N results obtained by the solver in several cases..... | 38 |
| Table 5.3 - C-27J Spartan C_L and C_D results obtained by the solver in several cases..... | 39 |
| Table 5.4 - C-130 Hercules C_L and C_D results obtained by the solver in several cases..... | 39 |
| Table 5.5 - Aerodynamic stability derivatives (values in rad^{-1})..... | 40 |
| Table 5.6 - Neutral point and static stability margin..... | 41 |

1. Introduction

1.1 Objectives

The objective of the thesis is the geometric modeling and analysis of performance, stability and control of two military transport turboprop aircraft. The airplanes analyzed in the following thesis are:

- C-27J Spartan;
- C-130 Hercules.

The geometric modeling was performed with the software JPAD Modeller, the performance with a MATLAB application while regarding the analysis of stability and control with the use of the solver VSPAERO.

1.2 Layout of work

Chapter 1: Introduction of the objectives and of the two aircraft.

Chapter 2: General description of aircraft components.

Chapter 3: JPAD Modeller and geometric modelling of the two aircraft.

Chapter 4: Analysis of performance of the two aircraft.

Chapter 5: Analysis of performance of the two aircraft.

Chapter 6: Conclusion and personal observations.

1.3 C-27J Spartan

The C-27J Spartan is a medium class military transport aircraft, used for missions of sending parachutists, equipment and medical aid. It was designed by Alenia Aeronautica and currently product by Leonardo Aircraft; the aircraft is supplied to the Italian Air Force and other countries such as Australia, Greece, Morocco and also by the American army. The version intended for the Italian Air Force is among the most complete presenting advanced data projection systems, protection systems for passive defense against surface-to-air missiles and probe for in-flight refueling. The C-27J Spartan is capable of carrying about sixty soldiers for missions and is characterized by two turboprop engines.



Figure 1.1- The Italian Air Force C-27J Spartan. [1]

1.4 C-130 Hercules

The C-130 Hercules is a military transport aircraft featuring 4 turboprop engines, used by USAF (United States Air Force) and other air forces for troop transport and material shipments. There are several versions of the aircraft, some used for war purposes, others in the meteorological field and for special missions. The C-130 Hercules can carry no more than ninety passengers, in fact the transport capacity is variable, depending on the mission and the purpose of the mission. It was produced by Lockheed, currently Lockheed Martin born from the union of the previous one with Martin Marietta in the mid-nineties.



Figure 1.2 – C-130 Hercules. [2]

2. Aircraft components

In this chapter of the thesis the aircraft main components will be analyzed, evaluating in a general way functions and characteristics of these. The components examined are:

- Fuselage;
- Wing;
- Tail;
- Engine.

2.1 Fuselage

The fuselage is the central body of the aircraft, and makes up most of the volume. It is used to transport payload, can contain fuel tanks and include the cockpit. Another function of the fuselage is to provide the necessary structure for the assembly of other components of the aircraft such as wings and tails. The important geometrical parameters are:

- Finess ratio $\frac{L}{D}$;
- Wet area.

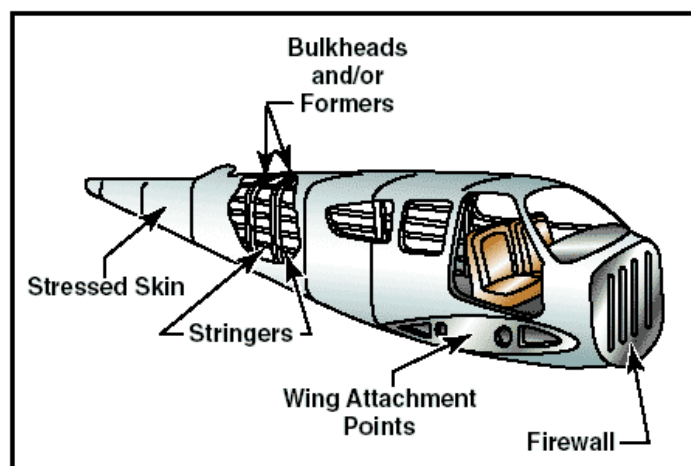


Figure 2.1 - Fuselage structure.

2.2 Wing

The wing is the main element of the aircraft that interacting with the relative air flow, generates the necessary lift to support the aircraft in flight. The wing also has the task of supporting the propulsion systems and contains a large part of the fuel; also has movable parts with control function (ailerons), aerobrakes (spoilers) and trailing-edge devices (flaps and slats).

2.2.1 Wing planform parameters

- Planform area S ;
- Wing span b ;
- Sweep angle Λ ;
- Root chord c_r ;
- Tip chord c_t ;
- Mean aerodynamic chord $\bar{c} = \frac{2}{S} \int_0^{\frac{b}{2}} c^2(y) dy$;
- Taper ratio $\lambda = \frac{c_t}{c_r}$;
- Aspect ratio $AR = \frac{b^2}{S}$;
- Dihedral angle Γ ;
- Aerodynamic twist angle ε_a ;
- Geometric twist angle ε_g .

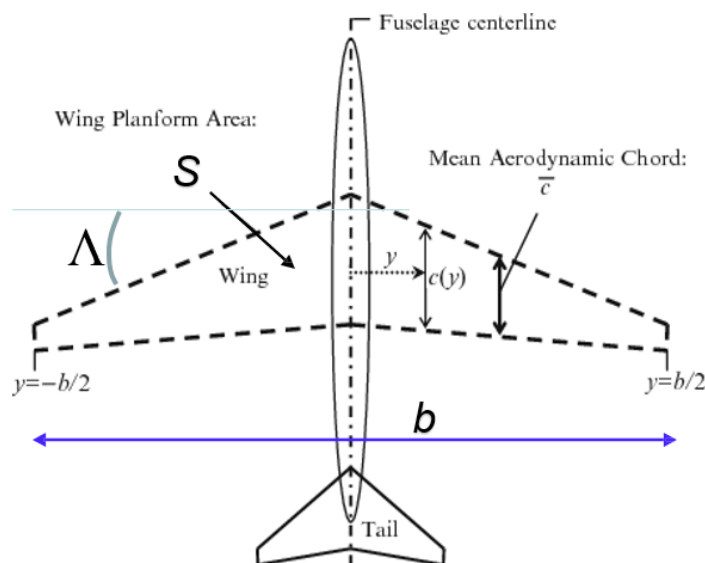


Figure 2.2 – Principal wing planform parameters. [3]



Figure 2.3 – Wing Dihedral angle. [3]

2.2.2 Ailerons

Ailerons are moving surfaces of the wing usually positioned on the trailing edge and contribute to lateral control. The pilot moving the cloche to the left or to the right activates ailerons:

- If the pilot moves the cloche to the left, the left aileron deflects upwards while the right aileron deflects downwards at same angle and rolling the aircraft to the left.
- If the pilot moves the cloche to the right, the right aileron deflects upwards while the left aileron deflects downwards always at same angle and rolling the aircraft to the right.



Figure 2.4 – Ailerons operation.

2.2.3 Flaps and Slats

The flaps are positioned on the trailing edge of the wing and allow to increase the generated lift by increasing the curvature of the wing profile. Instead, the slats, positioned on the leading

edge, have the function of delaying the separation of the air flow and therefore delaying the stall at high incidences. The flaps and slats allow to ensure stability even at low speeds and for these reasons these components are essential for the take-off and landing of the aircraft.

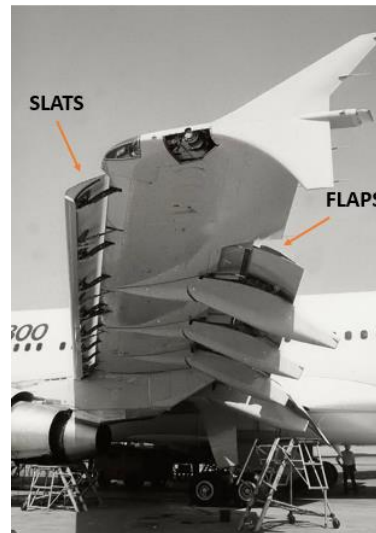


Figure 2.5 – Flaps and slats.

2.3 Tail

The tail is the aircraft surface with stabilizing functions and is characterized by one or more horizontal planes and at the same time by one or more vertical planes commonly known as horizontal tails and vertical tails respectively.

2.3.1 Horizontal Tail

The horizontal tail consists of a moving part and a fixed part, called respectively elevator and horizontal stabilizer, contributes in small part to the generation of lift and in an influential way to restore the stability at the pitch. Both components forming the horizontal tail are assembled at the back of fuselage. The elevator has the function of varying the lift of the tailplane favoring the inclination of the aircraft allowing the pitch while the horizontal stabilizer is a fixed surface assembled with the elevator.

2.3.2 Vertical Tail

The vertical tail also consists of a mobile part and a fixed part, called rudder and vertical stabilizer. It helps to restore lateral stability without generating lift. The rudder placed vertically

is operated by the rudder pedals that allows a rotation to the left or to the right of the rudder. As in the case of elevator-horizontal stabilizer, the vertical stabilizer is assembled with the rudder.

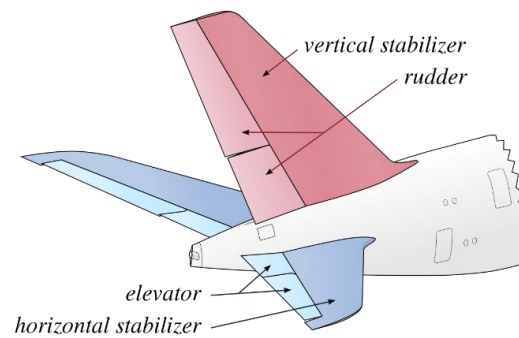


Figure 2.6 – Horizontal and vertical tails.

2.4 Engine

The motor by definition is a device capable of transforming an energy source, which for example can be in chemical, thermal or even electrical form, into mechanical energy. Aircraft engines are based by the propulsion principle, as a propulsion system is capable of generating a force on a fluid, involving the acceleration in a certain direction. To this force for the Third Principle of dynamics corresponds an equal and opposite one acting on the propulsive system itself. In other words, the propulsion system must provide the necessary thrust to flight, which is generated by the momentum variation.

$$T = m_a \frac{\Delta V}{\Delta t} = \dot{m}_a \Delta V \quad (2.1)$$

2.4.1 Turboprop engine

The two aircraft examined in the following thesis have turboprop engines, where the propulsion take place by the effect of the air set in motion thanks to a propeller and in small part by the exhaust gases thrust. Turboprop engines are characterized by a compressor, a combustion chamber and a turbine, which receiving energy from burnt gases, drives the propeller through a shaft and a gearbox. The turbine is used to operate the compressor.

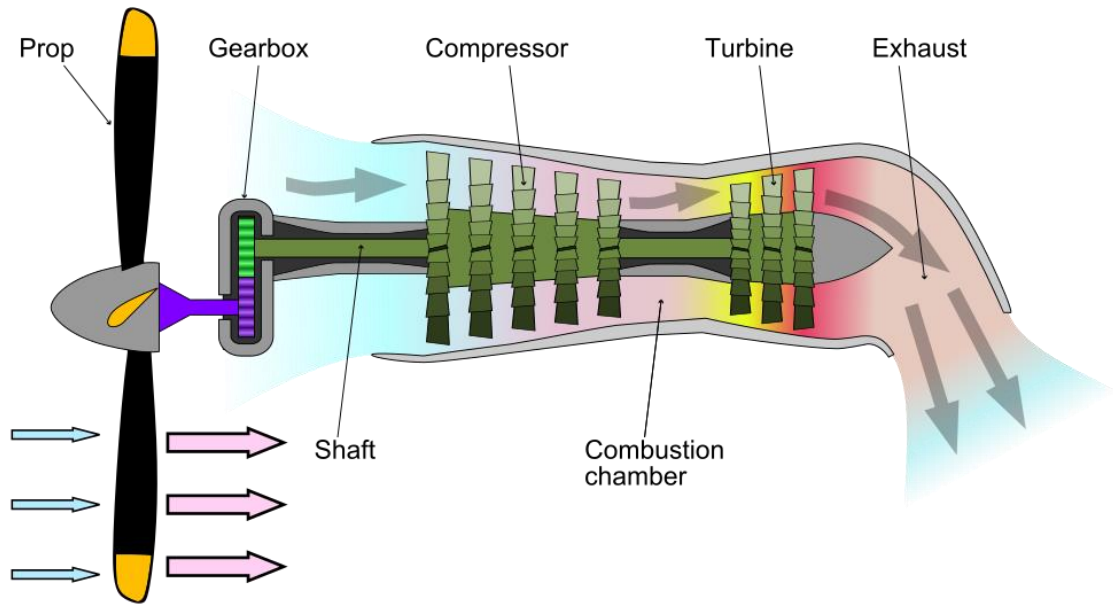


Figure 2.7 – Scheme of turboprop engine.

3. Geometric modelling

JPAD Modeller has been used for geometric modelling. JPAD Modeller is a software developed by SmartUp Engineering s.r.l. and is characterized by several useful features adopted for the study phases of conceptual and preliminary design of the aircraft. The following are some of the most important features of the software [4]:

- Statistical and conceptual design of conventional aircraft;
- User friendly UI to manage aircraft component CAD models;
- Automatic CAD models generation suitable for third-party CAD software;
- Export to OPENVSP and VSPAERO;
- Management of fairings and wing-fuselage configurations.

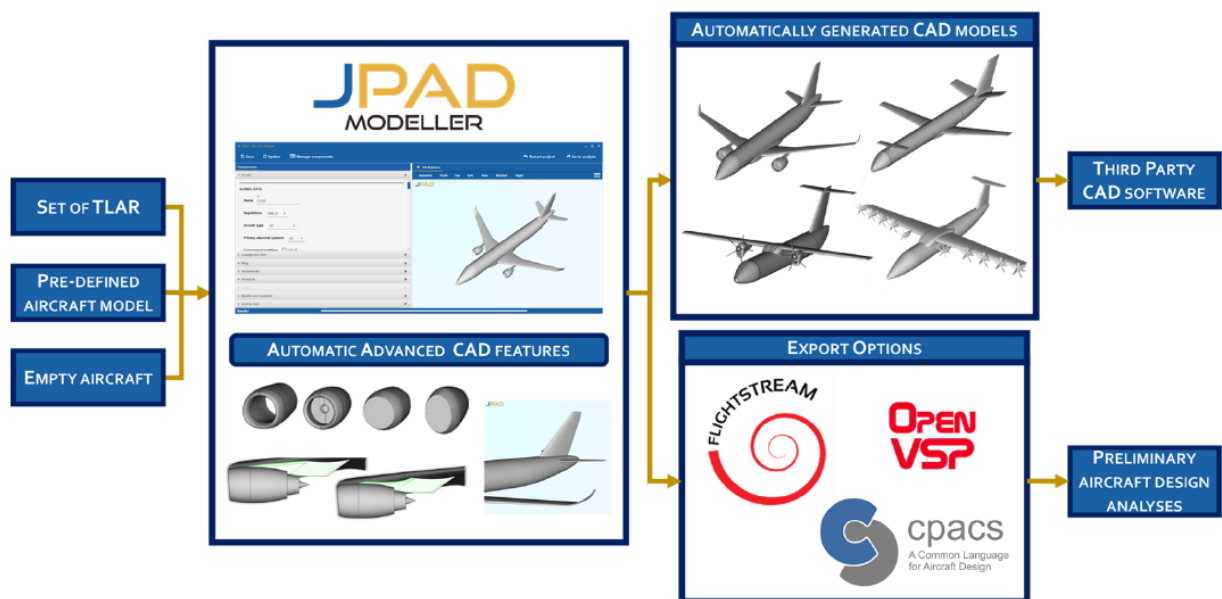


Figure 3.1 – JPAD Modeller key visual. [4]

3.1 Data

To perform the geometric modelling with JPAD Modeller, it is necessary to have some technical data of the aircraft that must be entered in the software and then proceed with the operations concerned. The tables in the two sub-paragraphs show some of the technical data of the two aircraft examined in the following thesis.

3.1.1 C-27J Spartan

Table 3.1 – C-27J Spartan technical data. [1],[5]

| | |
|----------------------------|---------------------------------|
| Length | 22.70 m |
| Height | 9.20 m |
| Planform area | 82 m ² |
| Wing span | 29.70 m |
| Empty Mass | 17000 kg |
| Total Mass | 31800 kg |
| Engine | 2 Turboprop Rolls-Royce 2100D2A |
| Engine Power (each) | 3457.81 kW (4637 shp) |
| Max. speed | 602 km/h |
| Range | 1852 km |
| Service Ceiling | 9100 km |

3.1.2 C-130 Hercules

Table 3.2 – C-130 Hercules technical data. [2],[5]

| | |
|----------------------------|--|
| Length | 29.30 m |
| Height | 11.90 m |
| Planform area | 162.12 m ² |
| Wing span | 39.70 m |
| Empty Mass | 34274 kg |
| Total Mass | 69750 kg |
| Engine | 4 Turboprop Rolls-Royce Allison T56-A-15 |
| Engine Power (each) | 3423.51 kW (4591 shp) |
| Max. speed | 890 km/h |
| Range | 5250 km |
| Service Ceiling | 9315 km |

3.2 Geometric modelling process

After starting JPAD Modeller, for the realization of the two aircraft CAD models there was a preliminary phase of software study during which the various main functionalities offered were observed and understood then proceed to generate the various components of the aircraft such as the wings, fuselage, tails, engines for some of them it was necessary to enter values from Table 3.1 for the first aircraft and Table 3.2 for the second. The positioning of the components took place using the coordinates X, Y, Z generating a first model for the two aircraft and for the components characterized by mobile surfaces were added the latter. To obtain more realistic models similar to their realistic counterparts, using the various views of the aircraft the models obtained were compared with the respective line drawings and thanks the continuous comparison further modifications were made both in coordinates and in the sizing of the various components creating the definitive models. Once obtained the two models, through JPAD Modeller it is possible to get approximate line drawings of the two aircraft and also to evaluate, for example, the operation of the mobile surfaces.

3.3 C-27J Spartan geometric modelling



Figure 3.2 – C-27J Spartan isometric view.

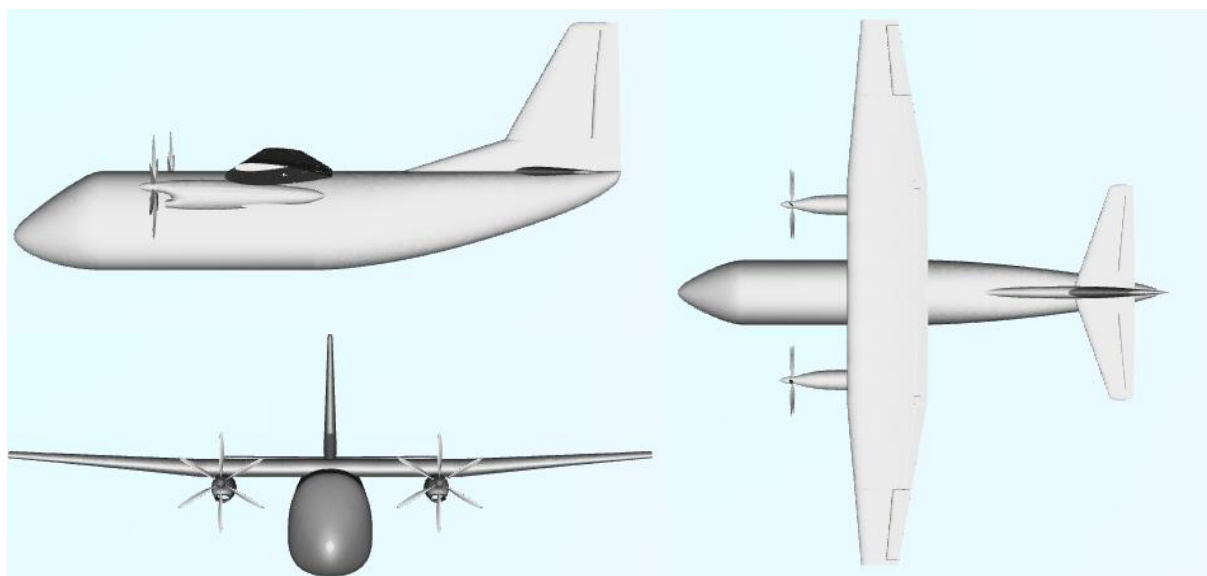


Figure 3.3 – C-27J Spartan CAD model views.

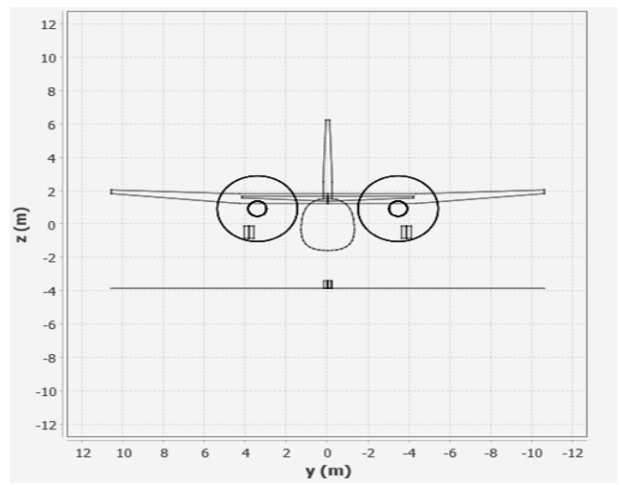
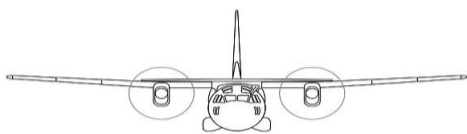
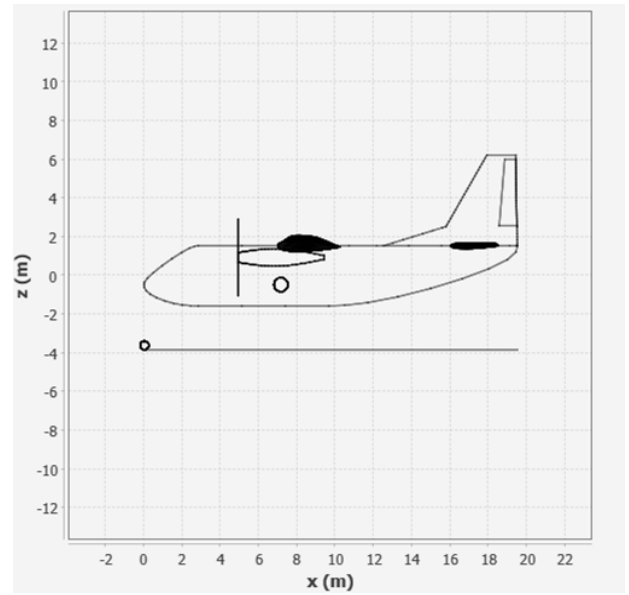
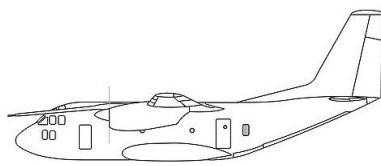
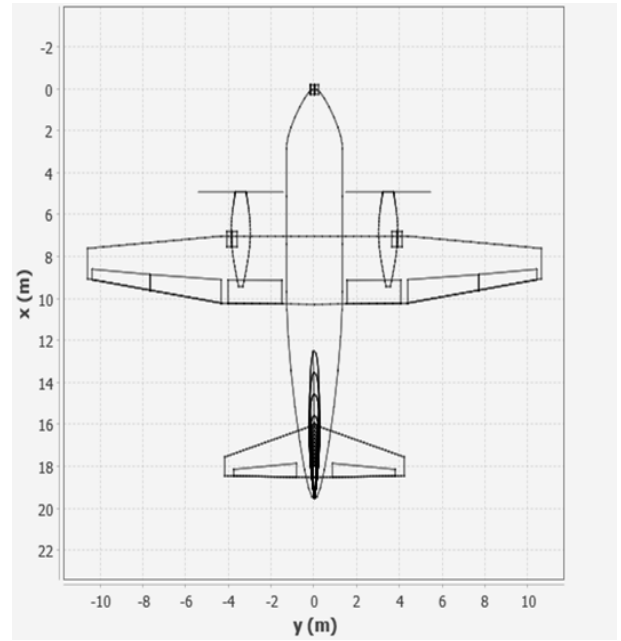
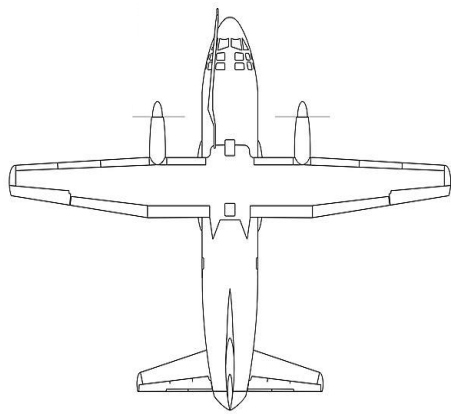


Figure 3.4 – Comparison of C-27J Spartan line drawings.

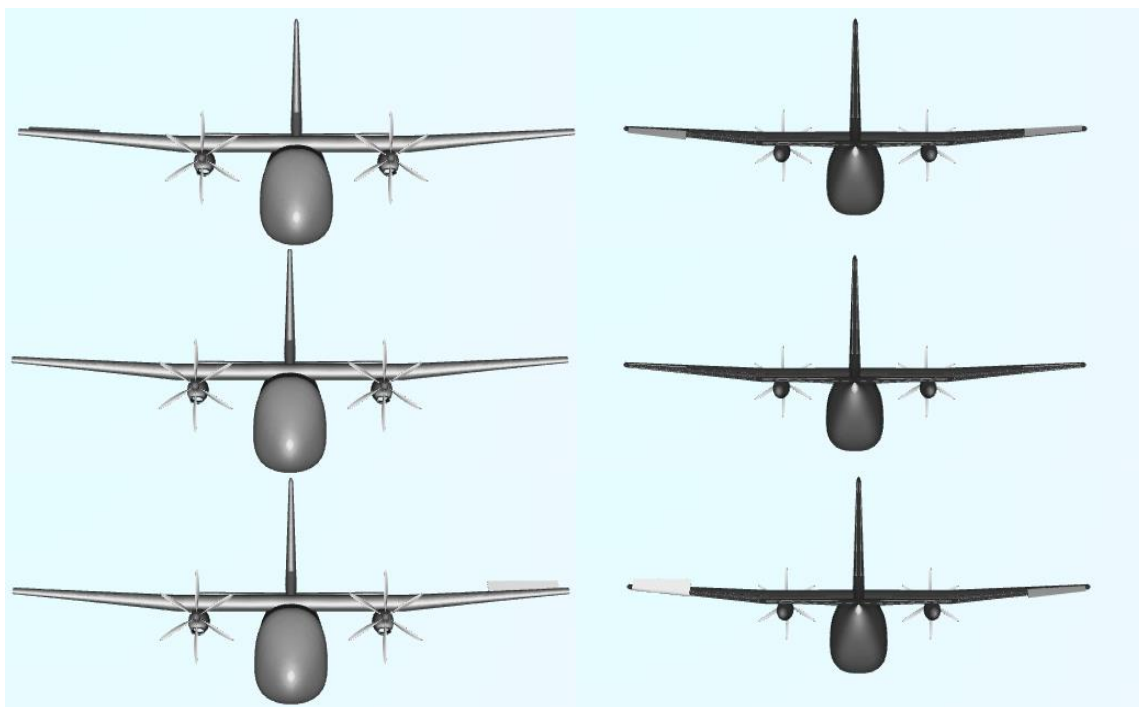


Figure 3.5 – C-27J Spartan ailerons operation (-25°, 0°, +25°).

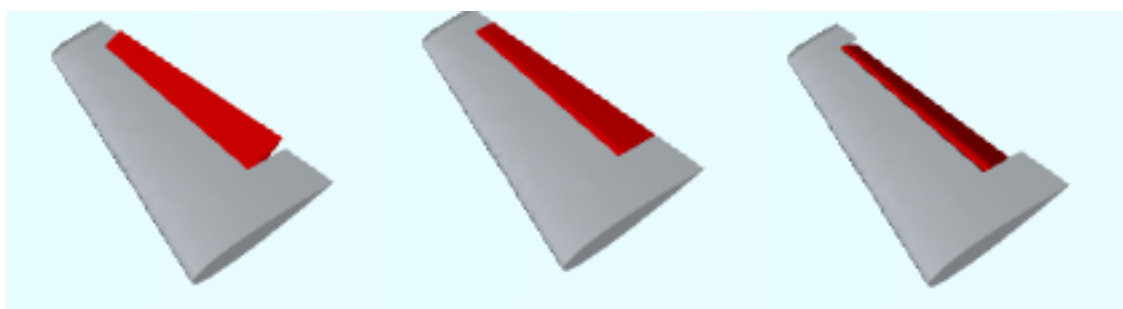


Figure 3.6 – C-27J Spartan elevator operation (-25°, 0°, +25°).

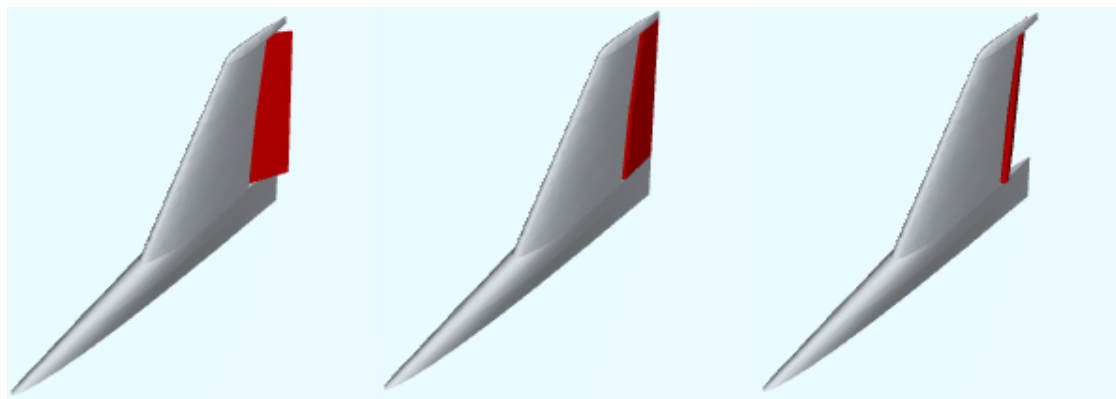


Figure 3.7 – C-27J Spartan rudder operation (-30°, 0°, +30°).



Figure 3.8 – C-27J Spartan flaps operation (0°, +45°).

3.4 C-130 Hercules geometric modelling

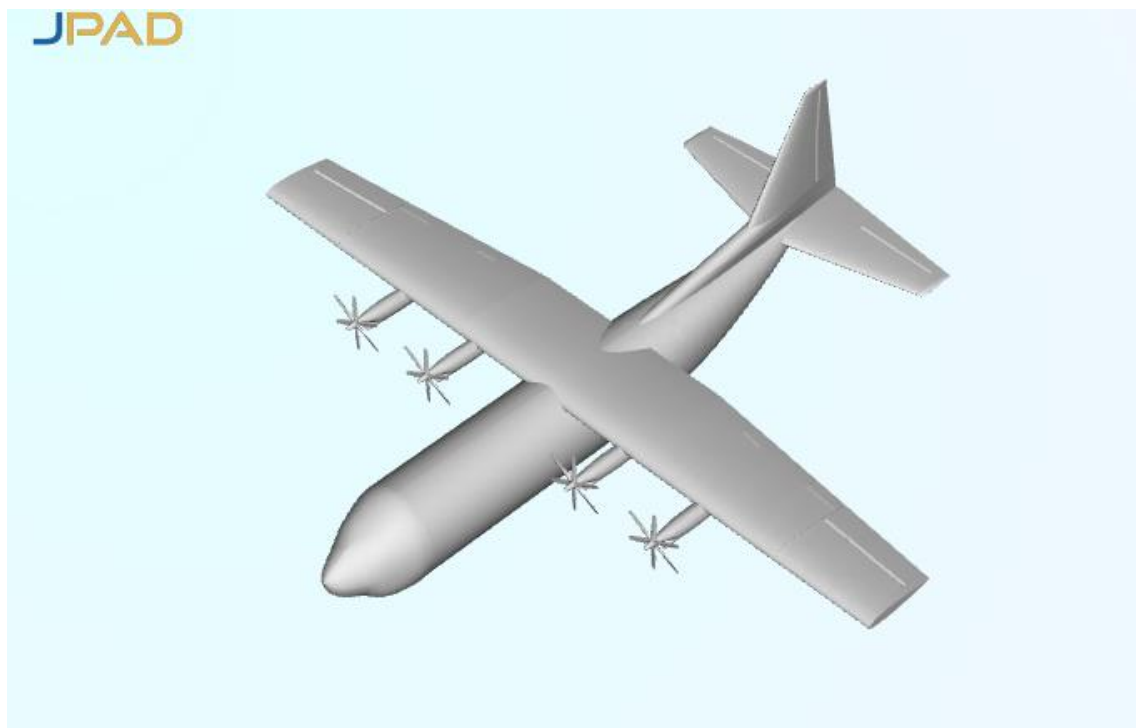


Figure 3.9 – C-130 Hercules isometric view.

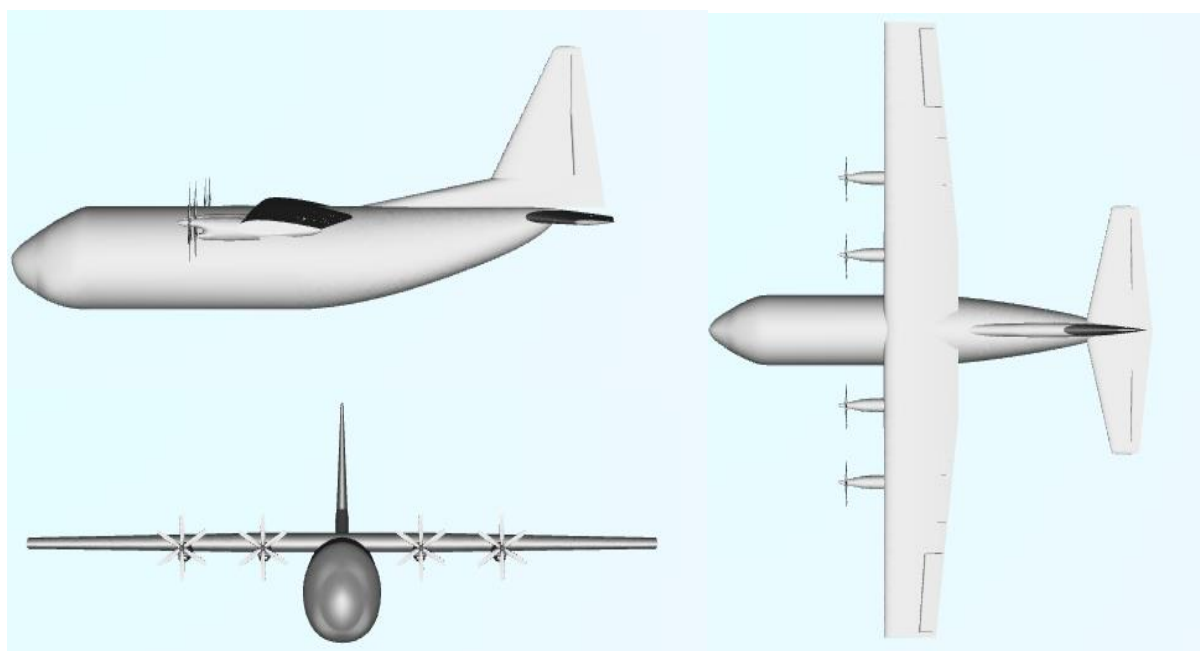


Figure 3.10 – C-130 Hercules CAD model views.

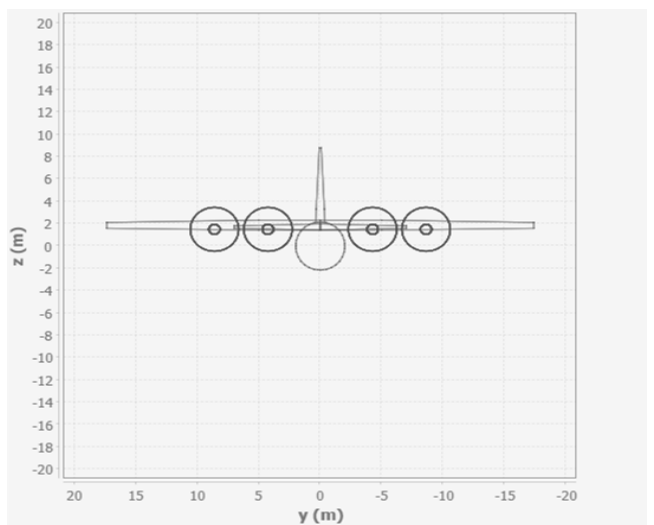
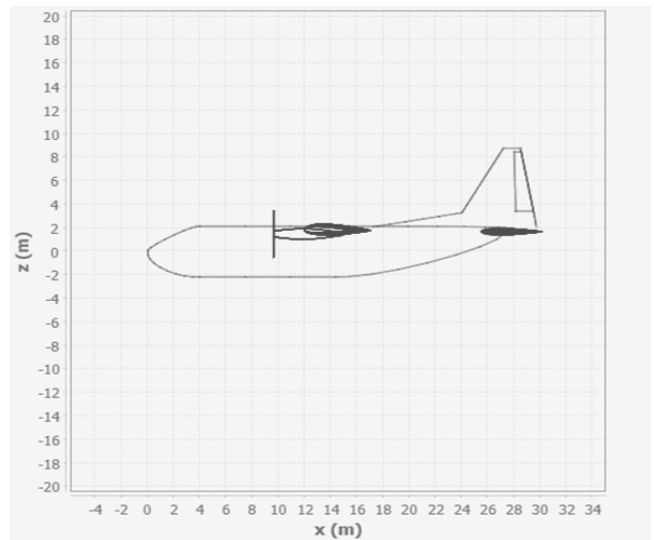
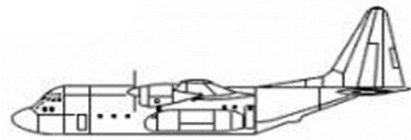
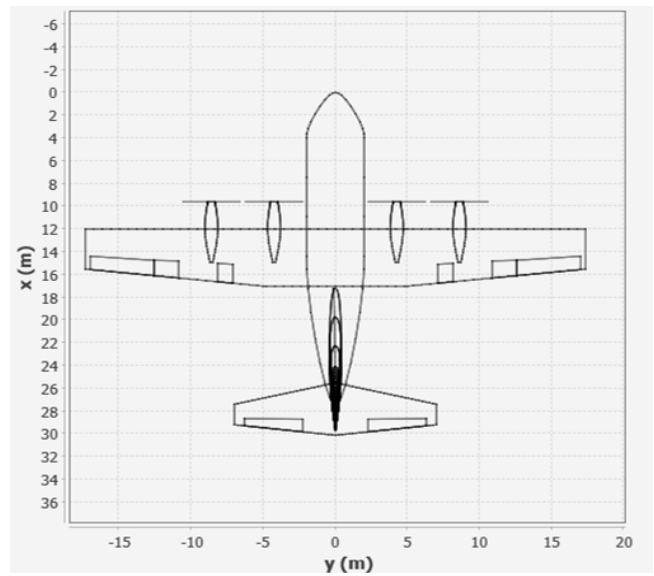
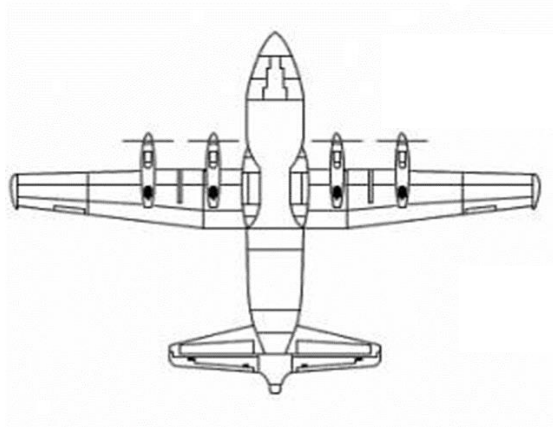


Figure 3.11 – Comparison of C-130 Hercules line drawings.

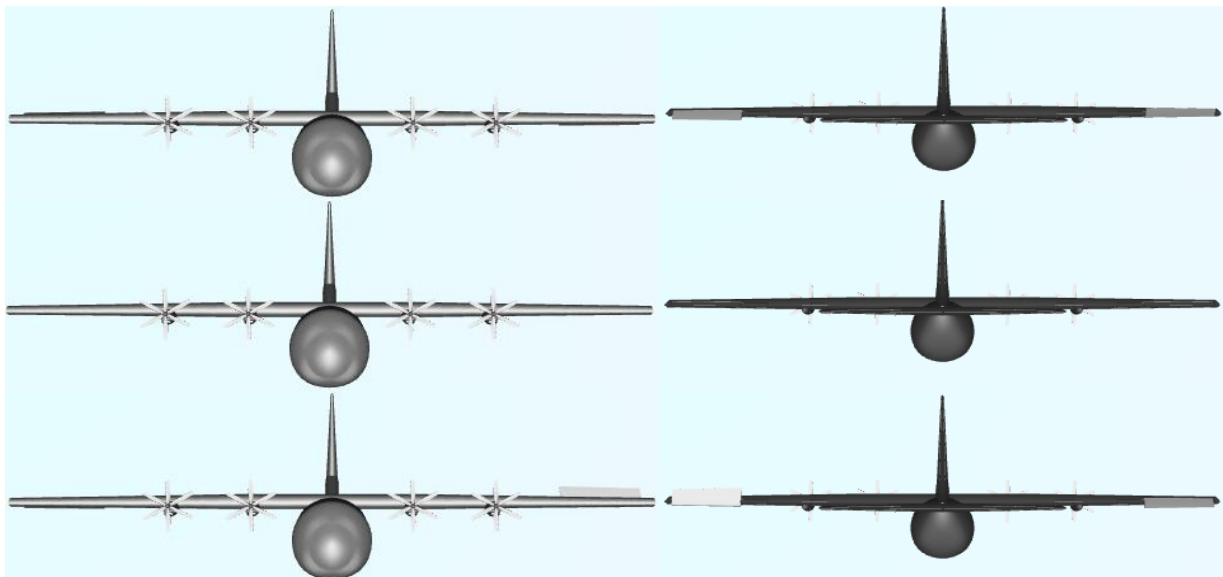


Figure 3.12 – C-130 Hercules ailerons operation (-25°, 0°, +25°).

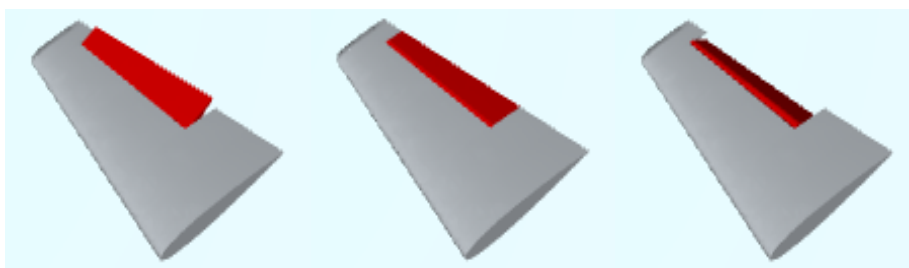


Figure 3.13 – C-130 Hercules elevator operation (-25°, 0°, +25°).



Figure 3.14 – C-130 Hercules rudder operation (-30° , 0° , $+30^\circ$).



Figure 3.15 – C-130 Hercules flaps operation (0° , $+45^\circ$).

4. Analysis of performance

After concluding the geometric modelling was carried out the analysis of performance of the two aircraft, that was performed through a MATLAB live script that outputs the different results of the various performances taken into consideration. To get the results from the script, it was necessary to create MATLAB codes where the values about sizing, capacity and propulsive characteristics of the two aircraft were entered; successively through technical procedures the codes have been implemented in such a way that they can be run in the live script. The results of the analysis of performance obtained have been reported in the following sub-paragraphs.

4.1 Input data

The following tables show the input data entered in the MATLAB codes to perform the analysis of performance, considering the following parameters:

- Load factor $n_{\max} = 2.5$;
- Sea Level = 0 m;
- Climb = 3500 m;
- Cruise = 7000 m;
- Selected Altitude = 5090 m.

Table 4.1 – Aerodynamic data.

Aerodynamic data

| <i>Aircraft</i> | C_{D0} | $C_{L\max}$ | e | $C_{L\max,TO}$ | $C_{L\max,L}$ | C_{Lg} |
|-----------------------|----------|-------------|------|----------------|---------------|----------|
| <i>C-27J Spartan</i> | 0.030 | 1.50 | 0.80 | 2.20 | 2.80 | 0.60 |
| <i>C-130 Hercules</i> | 0.030 | 1.50 | 0.80 | 2.20 | 2.80 | 0.60 |

Table 4.2 – Weight and Geometry data.

Weight and Geometry data

| <i>Aircraft</i> | W_{TO} [kg] | W_f [kg] | S [m²] | b [m] |
|-----------------------|----------------------------|---------------------------|--------------------------|--------------|
| <i>C-27J Spartan</i> | 31800 | 5440 | 82.0 | 29.7 |
| <i>C-130 Hercules</i> | 69750 | 18000 | 162.1 | 39.7 |

Table 4.3 – Powerplant data.

Powerplant data

| <i>Aircraft</i> | P₀ of a single engine [hp] | SFC [$\frac{lb}{lb \cdot hr}$] | n^o |
|-----------------------|--|--|----------------------|
| <i>C-27J Spartan</i> | 4637 | 0.49 | 2 |
| <i>C-130 Hercules</i> | 4591 | 0.49 | 4 |

4.2 Technical Polar

The characteristic points of the driving polar curve are:

- Point E;
- Point P;
- Point A;
- Point S.

The Point E is the point of maximum efficiency and the drag is minimum, the Point P is the point of minimum power in level flight while the Points A and S are respectively the condition that maximizes the Range and the point of minimum aircraft speed. The results and the graphs were calculated at sea level, climb (3500 m) and cruise (7000 m) flight altitudes.

Table 4.4 – Point E, Sea Level.
Sea Level
Point E

| <i>Aircraft</i> | C_L | C_D | E | $V \left[\frac{m}{s} \right]$ | T [N] | P [kW] | M |
|-----------------------|-------|--------|------|--------------------------------|-------|--------|------|
| <i>C-27J Spartan</i> | 0.90 | 0.0600 | 15.0 | 83.05 | 20783 | 1726 | 0.24 |
| <i>C-130 Hercules</i> | 0.86 | 0.0600 | 14.3 | 89.71 | 47953 | 4302 | 0.26 |

Table 4.5 – Point P, Sea Level.
Sea Level
Point P

| <i>Aircraft</i> | C_L | C_D | E | $V \left[\frac{m}{s} \right]$ | T [N] | P [kW] | M |
|-----------------------|-------|--------|------|--------------------------------|-------|--------|------|
| <i>C-27J Spartan</i> | 1.56 | 0.1200 | 13.0 | 63.10 | 23999 | 1514 | 0.19 |
| <i>C-130 Hercules</i> | 1.48 | 0.1200 | 12.4 | 68.17 | 55371 | 3775 | 0.20 |

Table 4.6 – Point A, Sea Level.
Sea Level
Point A

| <i>Aircraft</i> | C_L | C_D | E | $V \left[\frac{m}{s} \right]$ | T [N] | P [kW] | M |
|-----------------------|-------|--------|------|--------------------------------|-------|--------|------|
| <i>C-27J Spartan</i> | 0.52 | 0.0400 | 13.0 | 109.30 | 23999 | 2623 | 0.32 |
| <i>C-130 Hercules</i> | 0.49 | 0.0400 | 12.4 | 118.07 | 55371 | 6538 | 0.35 |

Table 4.7 – Point S, Sea Level.
Sea Level
Point S

| <i>Aircraft</i> | C_L | C_D | E | $V \left[\frac{m}{s} \right]$ | T [N] | P [kW] | M |
|-----------------------|-------|--------|------|--------------------------------|-------|--------|------|
| <i>C-27J Spartan</i> | 1.50 | 0.1132 | 13.3 | 64.35 | 23547 | 1515 | 0.19 |
| <i>C-130 Hercules</i> | 1.50 | 0.1221 | 12.3 | 67.78 | 55692 | 3775 | 0.20 |

Table 4.8 – Point E, Climb Level.

| <i>Climb Level</i> | | | | | | | |
|-----------------------|-------|--------|------|--------------------------------|-----------------|------------------|------|
| <i>Point E</i> | | | | | | | |
| <i>Aircraft</i> | C_L | C_D | E | $V \left[\frac{m}{s} \right]$ | $T \text{ [N]}$ | $P \text{ [kW]}$ | M |
| <i>C-27J Spartan</i> | 0.90 | 0.0600 | 15.0 | 98.93 | 20783 | 2056 | 0.30 |
| <i>C-130 Hercules</i> | 0.86 | 0.0600 | 14.3 | 106.87 | 47953 | 5125 | 0.33 |

Table 4.9 – Point P, Climb Level.

| <i>Climb Level</i> | | | | | | | |
|-----------------------|-------|--------|------|--------------------------------|-----------------|------------------|------|
| <i>Point P</i> | | | | | | | |
| <i>Aircraft</i> | C_L | C_D | E | $V \left[\frac{m}{s} \right]$ | $T \text{ [N]}$ | $P \text{ [kW]}$ | M |
| <i>C-27J Spartan</i> | 1.56 | 0.1200 | 13.0 | 75.17 | 23999 | 1804 | 0.23 |
| <i>C-130 Hercules</i> | 1.48 | 0.1200 | 12.4 | 81.21 | 55371 | 4496 | 0.25 |

Table 4.10 – Point A, Climb Level.

| <i>Climb Level</i> | | | | | | | |
|-----------------------|-------|--------|------|--------------------------------|-----------------|------------------|------|
| <i>Point A</i> | | | | | | | |
| <i>Aircraft</i> | C_L | C_D | E | $V \left[\frac{m}{s} \right]$ | $T \text{ [N]}$ | $P \text{ [kW]}$ | M |
| <i>C-27J Spartan</i> | 0.52 | 0.0400 | 13.0 | 130.20 | 23999 | 3125 | 0.40 |
| <i>C-130 Hercules</i> | 0.49 | 0.0400 | 12.4 | 140.65 | 55371 | 7788 | 0.43 |

Table 4.11 – Point S, Climb Level.

| <i>Climb Level</i> | | | | | | | |
|-----------------------|-------|--------|------|--------------------------------|-----------------|------------------|------|
| <i>Point S</i> | | | | | | | |
| <i>Aircraft</i> | C_L | C_D | E | $V \left[\frac{m}{s} \right]$ | $T \text{ [N]}$ | $P \text{ [kW]}$ | M |
| <i>C-27J Spartan</i> | 1.50 | 0.1132 | 13.3 | 76.66 | 23547 | 1805 | 0.23 |
| <i>C-130 Hercules</i> | 1.50 | 0.1221 | 12.3 | 80.74 | 55692 | 4497 | 0.25 |

Table 4.12 – Point E, Cruise Level.

| <i>Cruise Level</i> | | | | | | | |
|-----------------------|-------|--------|------|--------------------------------|-------|--------|------|
| <i>Point E</i> | | | | | | | |
| <i>Aircraft</i> | C_L | C_D | E | $V \left[\frac{m}{s} \right]$ | T [N] | P [kW] | M |
| <i>C-27J Spartan</i> | 0.90 | 0.0600 | 15.0 | 119.72 | 20783 | 2488 | 0.38 |
| <i>C-130 Hercules</i> | 0.86 | 0.0600 | 14.3 | 129.33 | 47953 | 6202 | 0.41 |

Table 4.13 – Point P, Cruise Level.

| <i>Cruise Level</i> | | | | | | | |
|-----------------------|-------|--------|------|--------------------------------|-------|--------|------|
| <i>Point P</i> | | | | | | | |
| <i>Aircraft</i> | C_L | C_D | E | $V \left[\frac{m}{s} \right]$ | T [N] | P [kW] | M |
| <i>C-27J Spartan</i> | 1.56 | 0.1200 | 13.0 | 90.96 | 23999 | 2183 | 0.29 |
| <i>C-130 Hercules</i> | 1.48 | 0.1200 | 12.4 | 98.27 | 55371 | 5441 | 0.31 |

Table 4.14 – Point A, Cruise Level.

| <i>Cruise Level</i> | | | | | | | |
|-----------------------|-------|--------|------|--------------------------------|-------|--------|------|
| <i>Point A</i> | | | | | | | |
| <i>Aircraft</i> | C_L | C_D | E | $V \left[\frac{m}{s} \right]$ | T [N] | P [kW] | M |
| <i>C-27J Spartan</i> | 0.52 | 0.0400 | 13.0 | 157.55 | 23999 | 3781 | 0.50 |
| <i>C-130 Hercules</i> | 0.49 | 0.0400 | 12.4 | 170.20 | 55371 | 9424 | 0.55 |

Table 4.15 – Point S, Cruise Level.

| <i>Cruise Level</i> | | | | | | | |
|-----------------------|-------|--------|------|--------------------------------|-------|--------|------|
| <i>Point S</i> | | | | | | | |
| <i>Aircraft</i> | C_L | C_D | E | $V \left[\frac{m}{s} \right]$ | T [N] | P [kW] | M |
| <i>C-27J Spartan</i> | 1.50 | 0.1132 | 13.3 | 92.76 | 23547 | 2184 | 0.30 |
| <i>C-130 Hercules</i> | 1.50 | 0.1221 | 12.3 | 97.70 | 55692 | 5441 | 0.31 |

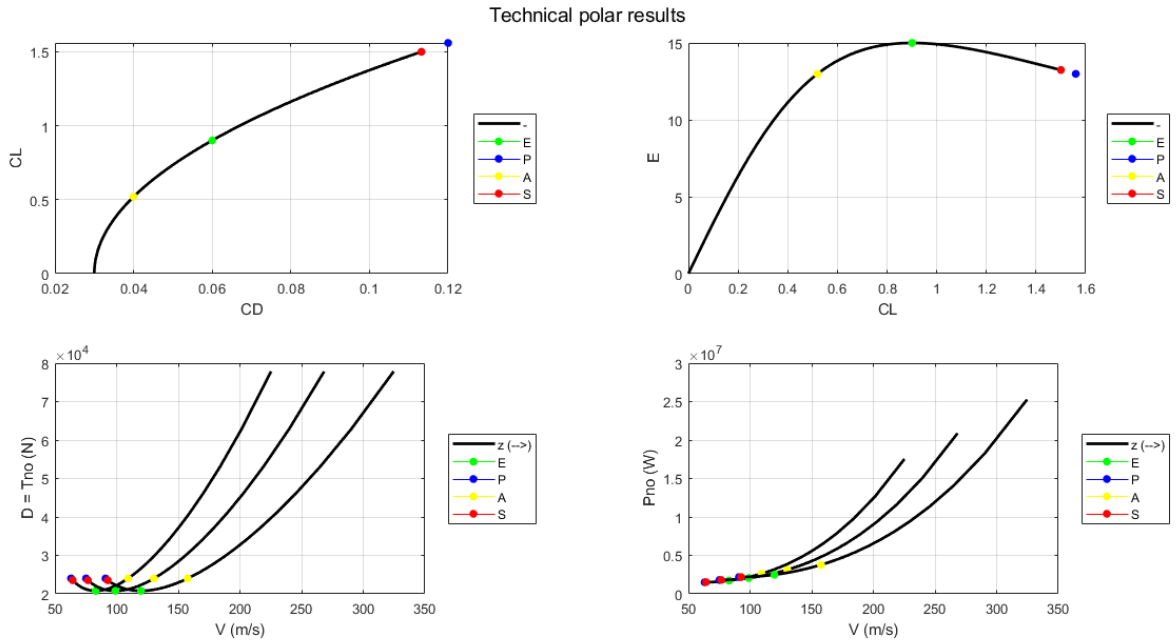


Figure 4.1 – C-27J Spartan Technical polar results.

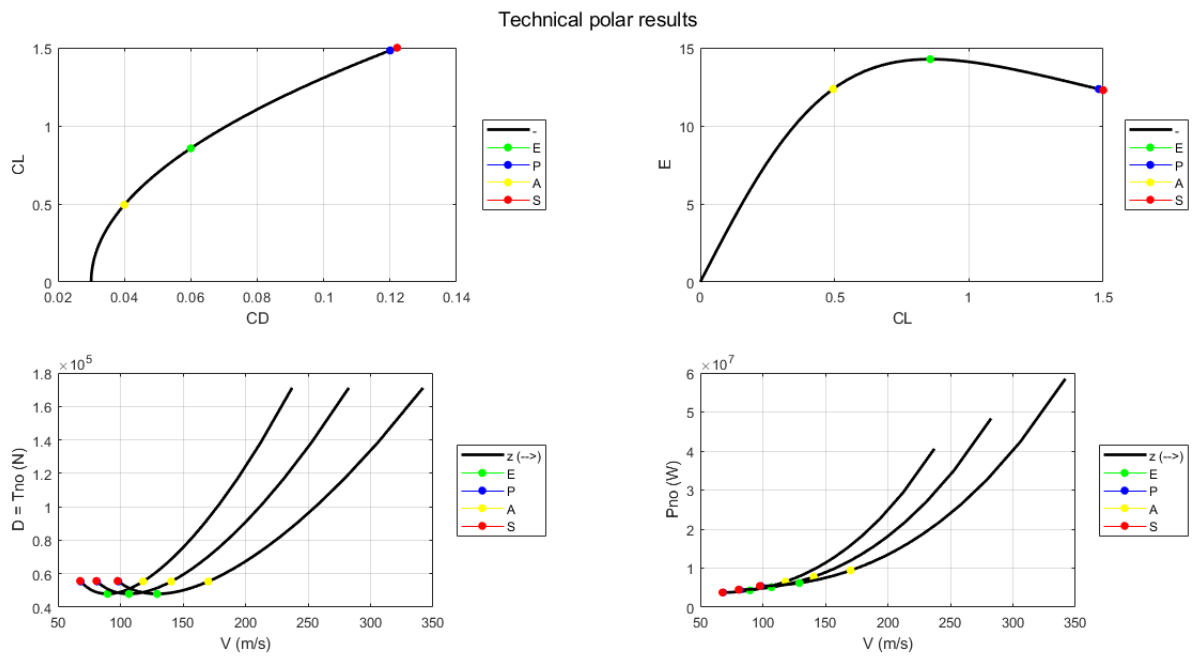


Figure 4.2 – C-130 Hercules Technical polar results.

4.3 Propulsive characteristics

These selected values were used for the calculation of propulsive characteristics:

- Throttle $\varphi = 1$;
- Flight time = 2.5 hr;
- Aircraft rating = Take off;
- VTAS = 125 m/s.

For the calculation of the performance, it was used the following rating:

$$P_A = P_{A0} \cdot \sigma \cdot \Phi \cdot KV \cdot n_{\text{engines}} \quad (4.1)$$

Aircraft propulsive characteristics in selected flight altitude condition are:

Table 4.16 – Propulsive Characteristics.

| <i>Aircraft</i> | T [kN] | P [kW] | Fuel [kg] |
|-----------------------|---------------|---------------|------------------|
| <i>C-27J Spartan</i> | 33 | 4065 | 3563.28 |
| <i>C-130 Hercules</i> | 64 | 8049 | 7055.87 |

4.4 Climb, level flight, autonomies, take-off and landing distances

For the calculation of the climb rate and endurance, an altitude of 5090 m and a speed of 125 m/s were used. These top performances are obtained in different conditions (altitude, airspeed, engine rating) and cannot occur all together.

Table 4.17 – Climb, level flight, autonomies, Take-off and Landing distances.

| <i>Aircraft</i> | RC_{max} [$\frac{m}{s}$] | V_{max} [$\frac{km}{h}$] | R_{max} [km] | En_{max} [hr] | Take-off field length [m] | Landing length [m] |
|-----------------------|--|--|-----------------------------|------------------------------|----------------------------------|---------------------------|
| <i>C-27J Spartan</i> | 4.33 | 547.07 | 2948 | 9.09 | 987 | 906 |
| <i>C-130 Hercules</i> | 2.91 | 505.40 | 4459 | 13.09 | 1261 | 923 |

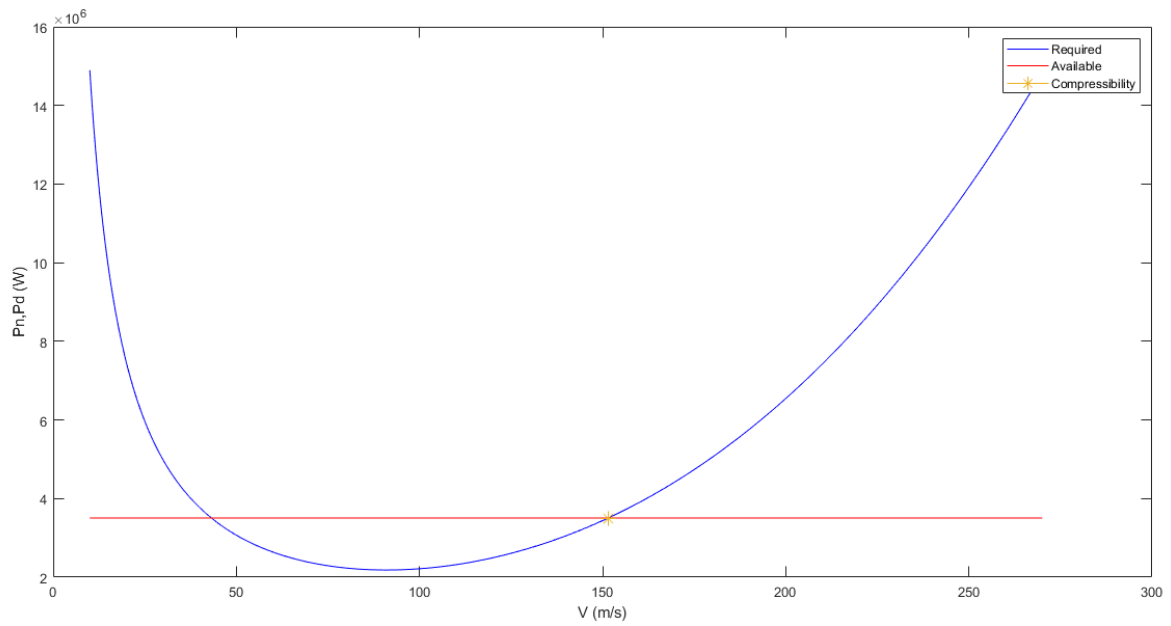


Figure 4.3 – C-27J Spartan diagram of required and available power.

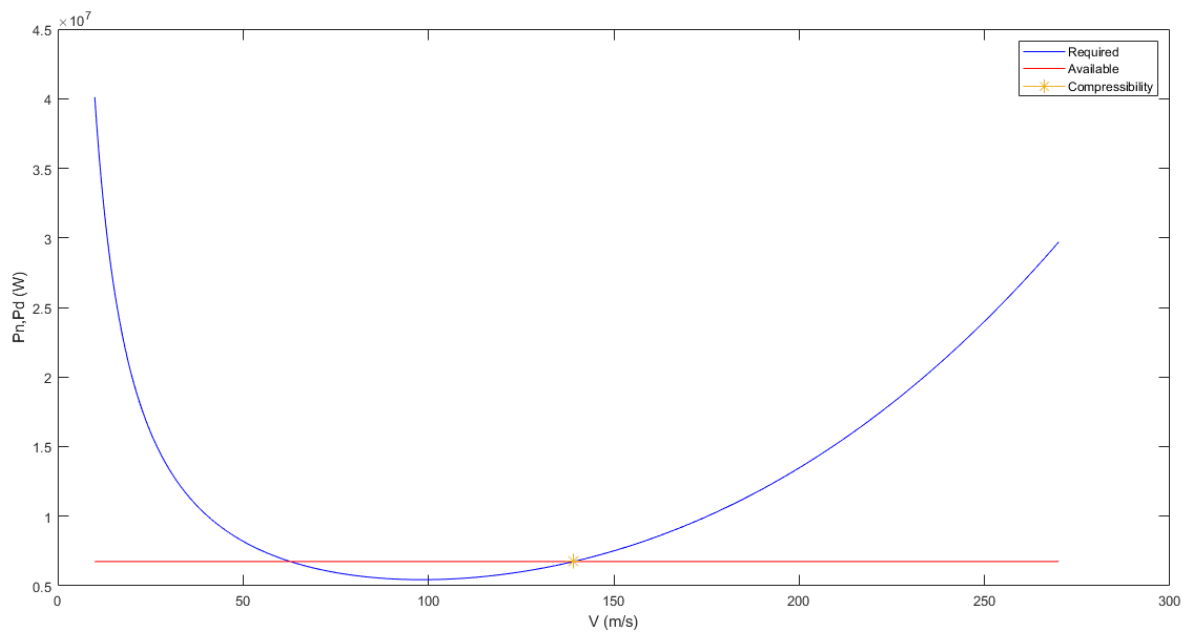


Figure 4.4 – C-130 Hercules diagram of required and available power.

4.5 Turn

In current conditions, the aircraft will make a turn with the following performance parameters:

- Turn speed = 115.00 m/s;
- Turn radius = 1622.94 m;
- Rate of turn = 4.06 deg/s;
- Bank angle = 39.72 deg.

The tables below show the best sustainable values with these performance parameters.

Table 4.18 – Turn.

| <i>Aircraft</i> | $V_{\min} [\frac{m}{s}]$ | $R_{\min} [m]$ | $RT_{\max} [\frac{deg}{s}]$ | Max Bank Angle [deg] | n_{\max} |
|-----------------------|--------------------------|----------------|-----------------------------|---------------------------------|------------|
| <i>C-27J Spartan</i> | 105.54 | 454.69 | 13.30 | 68.18 | 2.7 |
| <i>C-130 Hercules</i> | 102.97 | 519.58 | 11.36 | 64.33 | 2.3 |

5. Analysis of stability and control

Finally, after finishing both the geometric modelling and the analysis of performance, the analysis of stability and control was performed, to carry it out it was necessary to import the CAD models of the two aircraft from JPAD Modeller in OpenVSP using functions of the latter. OpenVSP is a parametric aircraft geometry tool. OpenVSP allows the user to create a 3D model of an aircraft defined by common engineering parameters. This model can be processed into formats suitable for engineering analysis [6]. Among the different OpenVSP analysis tools was used VSPAERO that allows to perform vortex latex and flight dynamic analysis.

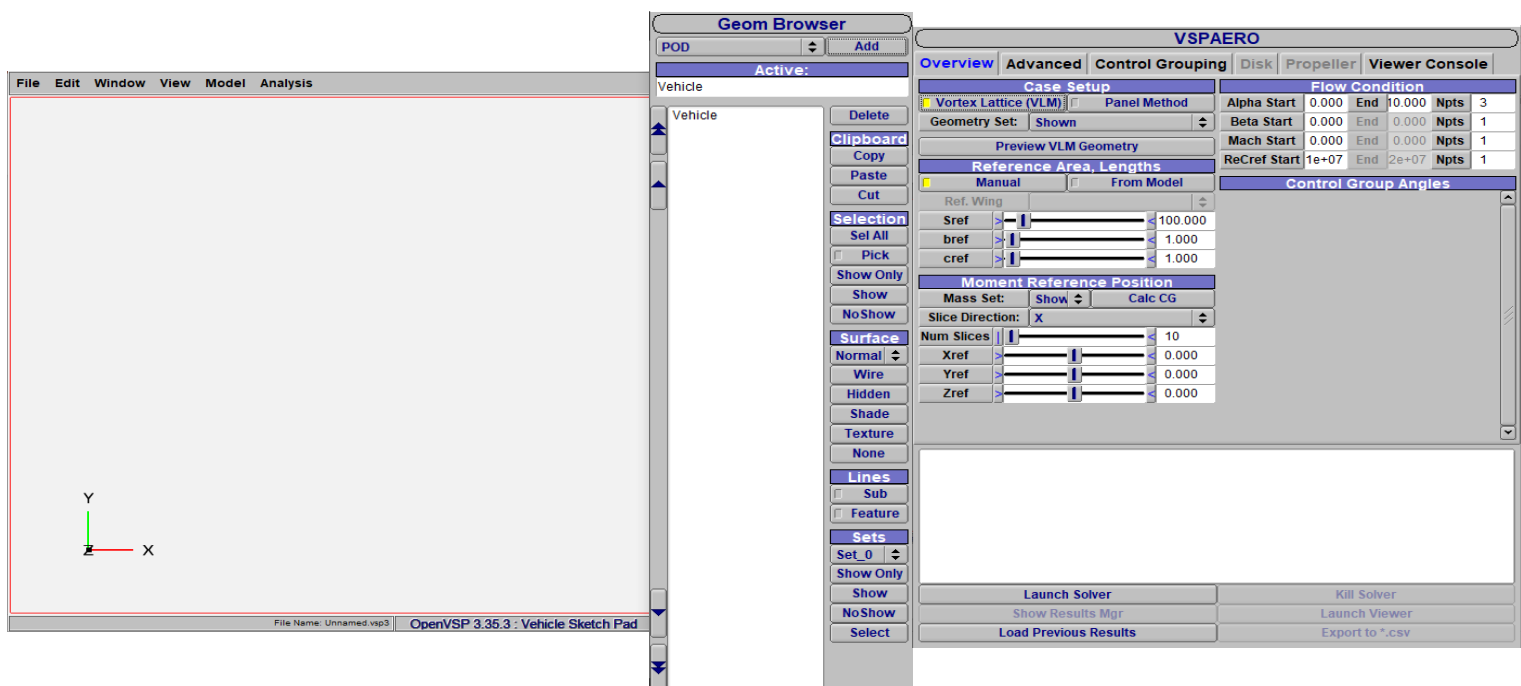


Figure 5.1 – OpenVSP user interface.

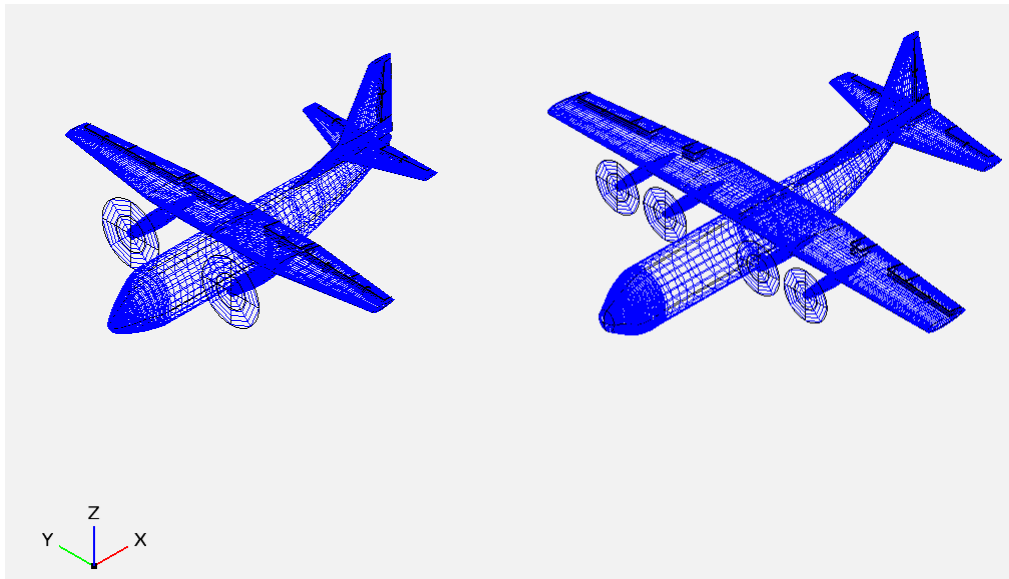


Figure 5.2 – The two aircraft models in OpenVSP.

VSPAERO has an interface where information about the aircraft and flight conditions can be entered and selected:

- “Vortex latex analysis” has been selected in “Case Setup”;
- In “Reference Area, Lengths” details about the size of the two aircraft were automatically obtained from OpenVSP;
- The y and z coordinates of the Center of Gravity were calculated automatically by the software while the x coordinate was inserted after having calculated it with the following equation:

$$x_{CG} = x_{Loc} + 0.30 c_r \quad (5.1)$$

where x_{Loc} is the leading-edge coordinate of the root chord c_r , both values always derived from the model. For C-27J Spartan $x_{CG} = 7.98$ while for the C-130 Hercules $x_{CG} = 13.50$.

VSPAERO does not require and does not return values with particular units of measurement, as it processes in terms of physical quantities. The input and output values were expressed considering the International System units of measurement.

- Three iterations have been set with the following flight conditions: variable angle of attack from 0° to 10° , Mach number at zero, Reynolds number at 1×10^7 and fixed movable surfaces.

The following tables show the values obtained for the two aircraft rolling, pitching and yaw moment coefficients (in order C_L , C_M , and C_N), the lift coefficient C_L and drag coefficient C_D in the different cases evaluated during the iterations.

Table 5.1 – C-27J Spartan C_L , C_M and C_N results obtained by the solver in several cases.

| C-27J Spartan | | | | | |
|------------------------------|----------------------------|--------------|-------------------------|-------------------------|-------------------------|
| Case | Δ | Units | C_L | C_M | C_N |
| Base Aero | +0.000 | n/a | 0.000 | 0.030 | 0.000 |
| α | +1.000 | Deg | 0.000 | -0.002 | 0.000 |
| β | +1.000 | deg | 0.000 | 0.030 | -0.005 |
| Roll Rate | +1.000 | rad/s | 0.053 | 0.034 | 0.001 |
| Pitch Rate | +1.000 | rad/s | 0.000 | -0.288 | 0.000 |
| Yaw Rate | +1.000 | rad/s | -0.010 | 0.037 | 0.030 |
| Mach | +0.100 | no unit | 0.000 | 0.030 | 0.000 |
| δ_a | +1.000 | deg | 0.003 | 0.030 | 0.000 |
| δ_e | +1.000 | deg | 0.000 | 0.000 | 0.000 |
| δ_r | +1.000 | deg | -0.001 | 0.030 | 0.002 |

Table 5.2 – C-130 Hercules C_L , C_M and C_N results obtained by the solver in several cases.

| C-130 Hercules | | | | | |
|------------------------------|----------------------------|--------------|-------------------------|-------------------------|-------------------------|
| Case | Δ | Units | C_L | C_M | C_N |
| Base Aero | +0.000 | n/a | 0.000 | 0.028 | 0.000 |
| α | +1.000 | deg | 0.000 | 0.000 | 0.000 |
| β | +1.000 | deg | 0.000 | 0.026 | -0.003 |
| Roll Rate | +1.000 | rad/s | 0.092 | 0.048 | 0.002 |
| Pitch Rate | +1.000 | rad/s | 0.000 | -0.442 | 0.000 |
| Yaw Rate | +1.000 | rad/s | -0.008 | 0.020 | 0.023 |
| Mach | +0.100 | no unit | 0.000 | 0.029 | 0.000 |
| δ_a | +1.000 | deg | 0.004 | 0.028 | 0.000 |
| δ_e | +1.000 | deg | 0.000 | 0.003 | 0.000 |
| δ_r | +1.000 | deg | 0.000 | 0.029 | 0.002 |

Table 5.3 – C-27J Spartan C_L and C_D results obtained by the solver in several cases.

| <i>C-27J Spartan</i> | | | | |
|----------------------|----------|---------|-------|-------|
| <i>Case</i> | Δ | Units | C_L | C_D |
| Base Aero | +0.000 | n/a | 0.061 | 0.011 |
| α | +1.000 | deg | 0.156 | 0.012 |
| β | +1.000 | deg | 0.062 | 0.011 |
| Roll Rate | +1.000 | rad/s | 0.061 | 0.003 |
| Pitch Rate | +1.000 | rad/s | 0.222 | 0.007 |
| Yaw Rate | +1.000 | rad/s | 0.059 | 0.007 |
| Mach | +0.100 | no unit | 0.061 | 0.011 |
| δ_a | +1.000 | deg | 0.061 | 0.011 |
| δ_e | +1.000 | deg | 0.070 | 0.011 |
| δ_r | +1.000 | deg | 0.061 | 0.011 |

 Table 5.4 – C-130 Hercules C_L and C_D results obtained by the solver in several cases.

| <i>C-130 Hercules</i> | | | | |
|-----------------------|----------|---------|-------|--------|
| <i>Case</i> | Δ | Units | C_L | C_D |
| Base Aero | +0.000 | n/a | 0.085 | 0.011 |
| α | +1.000 | deg | 0.180 | 0.012 |
| β | +1.000 | deg | 0.086 | 0.011 |
| Roll Rate | +1.000 | rad/s | 0.069 | -0.010 |
| Pitch Rate | +1.000 | rad/s | 0.344 | 0.000 |
| Yaw Rate | +1.000 | rad/s | 0.088 | 0.001 |
| Mach | +0.100 | no unit | 0.086 | 0.011 |
| δ_a | +1.000 | deg | 0.085 | 0.011 |
| δ_e | +1.000 | deg | 0.094 | 0.011 |
| δ_r | +1.000 | deg | 0.085 | 0.011 |

5.1 Aerodynamic stability derivatives

VSPAERO is able to evaluate the stability derivatives, to enable this it was necessary to select the section “Advanced”, always set three iterations, select as type of stability “Steady”, V_∞ at 100 m/s and density at 1.225 kg/m^3 . In addition, VSPAERO also allows to evaluate the control derivatives by selecting the moving surfaces (in these evaluations ailerons, elevator and rudder) and setting according to the right conventions the deflection gains per surface.

These derivatives indicate the variation of aerodynamic forces and moments represented by dimensionless coefficients with respect to state parameters. Here are the ones analyzed:

- Derivative of lift with respect to angle of attack $\frac{dC_L}{d\alpha}$;
- Derivative of pitch moment with respect to angle of attack $\frac{dC_M}{d\alpha}$;
- Derivative of roll moment with respect to sideslip angle $\frac{dC_L}{d\beta}$;
- Derivative of yaw moment with respect to sideslip angle $\frac{dC_N}{d\beta}$;
- Derivative of roll moment with respect to aileron deflection angle $\frac{dC_L}{d\delta_a}$;
- Derivative of pitch moment with respect to equilibrator deflection angle $\frac{dC_M}{d\delta_e}$;
- Derivative of yaw moment with respect to rudder deflection angle $\frac{dC_N}{d\delta_r}$.

The first four are stability derivatives while the remaining three are control derivatives. Below the table with the results obtained for the two aircraft.

Table 5.5 – Aerodynamic stability derivatives (values in rad^{-1}).

| <i>Aircraft</i> | $\frac{dC_L}{d\alpha}$ | $\frac{dC_M}{d\alpha}$ | $\frac{dC_L}{d\beta}$ | $\frac{dC_N}{d\beta}$ | $\frac{dC_L}{d\delta_a}$ | $\frac{dC_M}{d\delta_e}$ | $\frac{dC_N}{d\delta_r}$ |
|-----------------------|------------------------|------------------------|-----------------------|-----------------------|--------------------------|--------------------------|--------------------------|
| <i>C-27J Spartan</i> | 5.445 | -1.830 | 0.089 | -0.258 | 0.172 | -1.717 | 0.153 |
| <i>C-130 Hercules</i> | 5.441 | -1.629 | 0.023 | -0.143 | 0.210 | -1.479 | 0.093 |

5.2 Neutral point and static stability margin

At the end of the iterations, the neutral point x_N and the static stability margin SM are returned. By definition, the neutral point is the position of the Centre of Gravity that respects the neutral stability conditions; the expression for calculating the neutral point dimensionless with respect to mean aerodynamic chord is:

$$\bar{x}_N \equiv \frac{x_N}{\bar{c}} = \frac{\bar{x}_{ac,WB} + \eta_H \frac{C_{L\alpha,H}}{C_{L\alpha,WB}} \frac{S_H}{S} \bar{x}_{ac,H} \left[1 - \left(\frac{d\epsilon}{d\alpha} \right)_H \right]}{1 + \eta_H \frac{C_{L\alpha,H}}{C_{L\alpha,WB}} \frac{S_H}{S} \left[1 - \left(\frac{d\epsilon}{d\alpha} \right)_H \right]} \quad (5.2)$$

From which derives the equation for the static stability margin:

$$SM = \bar{x}_{CG} - \bar{x}_N \quad (5.3)$$

The static stability margin is a design requirement and stable aircraft has $x_{CG} < x_N$, hence $\frac{dC_M}{d\alpha} < 0$ and a static stability margin $SM < 0$.

Table 5.6 – Neutral point and static stability margin.

| <i>Aircraft</i> | SM | x_{CG} [m] | x_N [m] |
|-----------------------|-----------|---------------------------|--------------------------|
| <i>C-27J Spartan</i> | -0.34 | 7.98 | 8.91 |
| <i>C-130 Hercules</i> | -0.30 | 13.50 | 14.89 |

6. Conclusion

The purpose of the work was the geometric modelling, analysis of performance, stability and control of two turboprop transport military aircraft: the C-27J Spartan and the C-130 Hercules. The models' geometries, later used also for the analysis of stability and control, were made with JPAD Modeller. The analysis of performance was done in MATLAB, while the analysis of stability and control was performed with OpenVSP and the VSPAERO solver. The realization of the two models was the longest phase of the work, because it was necessary to design the final models starting from a simple cylinder. Thus, initially sketched models were created also to develop a proficiency in the software use to improve the definitive models' geometries. These are similar to the real counterparts within the limits of the JPAD Modeller. For the analysis of performance, it was sufficient to fill the MATLAB input data files of the two aircraft and execute a live script that was made available by the supervisor. Finally, the stability and control analysis in VSPAERO was initiated by exporting the geometric models from JPAD Modeller into the OpenVSP format. The execution of the aerodynamic solver VSPAERO provided the coefficients of aerodynamic forces and moments and their derivatives with respect to the flight variables (angle of attack and sideslip) and control variables (deflection angle of the control surfaces). The aerodynamic derivatives, representing the stability and control characteristics of the two airplanes, were reported in the tables at the end of this work. This work has provided Flight Mechanics data of two of the most famous, propeller-driven, military transport aircraft.

Bibliography

- [1] Aeronautica Militare. URL <https://www.aeronautica.difesa.it/2023/05/23/c-27j-spartan/>.
- [2] Air Force URL <https://www.af.mil/About-Us/Fact-Sheets/Display/Article/1555054/c-130-hercules/>.
- [3] Nicolosi, F. Corso di MECCANICA DEL VOLO modulo Prestazioni.
- [4] JPAD Modeller URL <https://www.smartup-engineering.com/jpad-modeller>.
- [5] Wikipedia URL <https://it.wikipedia.org>.
- [6] OpenVSP URL <https://openvsp.org>.

Ringraziamenti

Mi è doveroso dedicare questo spazio dell'elaborato alle persone che hanno contribuito, con il loro instancabile supporto, alla realizzazione dello stesso.

In primis, un ringraziamento al mio relatore il Prof. Danilo Ciliberti, per la sua grandissima disponibilità e per tutto l'aiuto fornito durante il percorso di stesura dell'elaborato.

Ringrazio infinitamente la mia famiglia: Mamma, Papà, Livia e il mio cagnolino Rudy; i miei primi tifosi sempre pronti a sostenermi e appoggiarmi in tutto, i primi a darmi una parola di conforto per un esame andato male, i primi a credere in un'impresa ritenuta da me impossibile, i primi con cui ho festeggiato l'arrivo a questo fantastico traguardo.

Vorrei ringraziare la mia comitiva: Serafino, Giancarlo e Salvatore. Serafino un fratello acquisito per me visto che ci conosciamo da molti anni, Giancarlo e Salvatore, conosciuti più recentemente ma due grandissimi simpaticoni, tutti e tre che mi hanno sempre sostenuto e continueranno a farlo anche nelle nuove sfide che mi attenderanno da qui in avanti.

Un pensiero lo vorrei dedicare ai miei nonni Rosa, Ciro e Guido che da lassù sarebbero orgogliosi di vedermi in questo momento realizzare il mio sogno da bambino, seppur io e nonno Guido non ci siamo mai incontrati ma credo che ne sarebbe fiero, e a nonna Livia che mi incoraggia sempre e a dare il massimo.

Ringrazio di cuore colleghi, anzi amici universitari che ho avuto modo di conoscere durante questo percorso anche all'ultimo esame, con cui tra una chiacchierata e un'altra ho avuto modo di confrontarmi, dare e ricevere supporto, divertirmi e arrivare fino in fondo al mio percorso universitario.

Un grazie speciale a tutti gli amici, le amiche e i parenti che mi hanno visto crescere, maturare e ora anche laurearmi.

Infine dulcis in fundo, vorrei dedicare questo traguardo a me stesso, sperando possa essere l'inizio di una lunga e brillante carriera professionale.